

Chapter - 6

Experimental Analysis of Radiator with Engine Assembly using Various Coolants

This chapter is divided into two sections. First section deals with the experimental performance evaluation of radiator cooling system, assembled with engine, for radiator coolants water, 25%PG brine and 25%EG brine. Second section deals with performance evaluation with optimum PG brine based hybrid nanofluids as new radiator coolant. The effects on radiator size, weight and cost, engine efficiency, fuel consumption and fuel energy distribution through various coolants have been discussed.

An automobile radiator cooling system is the collection of mechanical devices like pumps, heat exchanger, blower, coolants, that work together to maintain the engine temperature at optimal level. The cooling system essentially comprises passages inside the engine block and heads, a pump to circulate the coolant, a thermostat to control the flow of the coolant, a radiator to cool the coolant and a radiator cap controls the pressure within the system. In order to achieve the desired cooling action, the system circulates the liquid coolant through passages in the engine block and heads.

6.1 Experimental set up with engine assembly

This engine assembly based radiator cooling system comprises of automobile radiator (Maruti 800), water pump, measuring instruments, necessary piping and auxiliaries. The engine chosen for present experimentation is a single cylinder, four stroke, vertical, water cooled, direct injection Kirloskar made CI

Engine with hydraulic dynamometer and the engine specification (DI) with radiator as shown in Table-6.1.

An absorbing dynamometer acts as a load source that is driven by the prime mover and is able to operate at speed (Max.1500RPM) and load (Max. 6 kg) to any level of torque that the test requires. Also, it can be used to determine the torque and power required to operate a driven machine. The radiator set up consists of coolant tank of 10 litre capacity, pump, rotameter for flow measurement, inlet and outlet pipe accessories for engine and radiator inlet and outlet.

6.2 Experimental Methodology

8 litre of brine solution has to be prepared with 25 % PG (2litre) in 6 litre of water as radiator coolant and using the same procedure, 25% EG brine for coolant is prepared. All the thermo physical properties of the coolants such as density, conductivity, viscosity and specific heat are also measured in the laboratory mentioned in Chapter 3. Also, the dimensions of the radiator have been measured in the laboratory.

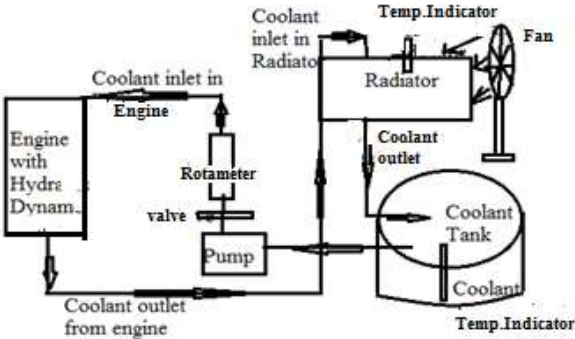


Figure 6.1: Schematic of Experimental Setup of engine cooling system

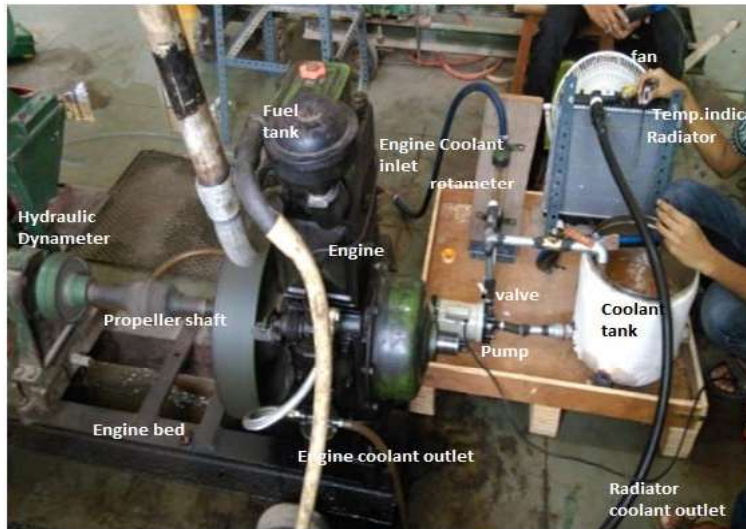


Figure 6.2 Photograph of Cooling System with Engine

Schematic diagram and fully instrumented experimental setup of radiator with engine assembly have been shown in Figs.6.1-6.2. After assembling the components of the radiator set up, the prepared coolant is supplied to insulated hot water storage tank of total volumetric capacity of 10 litres, in order to supply the coolants to the engine through pump and rotameter. A magnetic flow meter and valve were used to control and manipulate the flow rate with the precision of 0.2 l/min. K type thermocouples have been used in the flow line to record radiator fluid inlet, outlet temperatures and digital thermometer with PT 100 sensor is used to measure the inlet and outlet air temperatures flowing through the radiator at different loads applied to engine through hydraulic dynamometer. Anemometer was used to measure the frontal air velocity of the radiator.

Readings were taken at constant engine speed, constant flow rate & variable load i.e speed of 1500 rpm, flow rate of 8 lpm, velocity of air 4.5 m/s and various engine load 0 kg, 3 kg, 4.5 kg, 6 kg respectively representing no load, 1/2 load, 3/4 load and full load. For inlet air temperature of 35°C and coolant inlet temperature of 65°C, the overall heat transfer in radiator has been calculated



Figure 6.3: Coolant Temp.

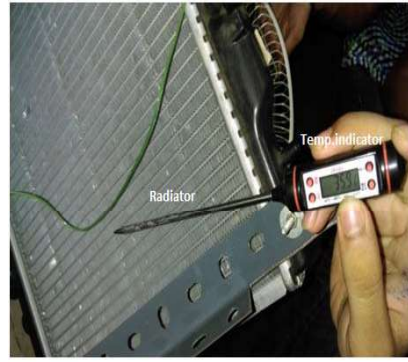


Figure 6.4 :Fin side Temp.

Measuring devices are shown in Table- 6.2 and Table- 6.3. On the basis of various engine parameters the effect of radiator heat transfer rate has been shown for water, PG brine, EG brine, nanofluid and hybrid nanofluids as radiator coolants.

Table 6.1: Engine and Radiator Specifications

Make & Model	Kirloskar CI Engine
Engine Details	Four stroke, CI, water cooled, DI engine.
No. of cylinder	One
Bore	80 mm
Stroke	110 mm
Compression ratio	16.5:1
Max. Power	5 bhp
Related speed	1500 rpm
Radiator Details	Rectangular fin radiators
Core dimension	0.321*0.33*.018 m ³
Tube size	16.4*2*321mm ³
No of tubes	33
Operating Conditions	Radiator
Water inlet Temp.	70°C
Air inlet Temp.	35°C
Coolant flow rate	8 lpm
Velocity of air	4.5m/s

Table- 6.2: Instrumentation and measuring devices

Thermo couple (K-Type) , Digital thermometer	Temperature
Hydraulic dynamometer (EEEG-301)	Engine load variation
Anemometer (LD AM-4201)	Air velocity
Tachometer (Victor DM6235P)	Engine Speed

Table -6.3: Measuring Parameters

Radiator	Temperature of water and air circuit, Air velocity, Coolant flow rate
Engine	Engine Fuel consumption, BSFC, Power of engine output, Engine speed.

6.3 Evaluation of radiator performance

The average heat transfer rate can be calculated as

$$Q_{avg} = \frac{Q_a + Q_c}{2} \quad (6.1)$$

Where Q_a and Q_c are the heat transfer rates at the air and the coolant stream, respectively.

The air-side and coolant side heat transfer rates can be calculated as

$$Q_a = m_a * c_{pa} * \Delta t_a \quad (6.2)$$

$$Q_c = m_c * c_{pc} * \Delta t_c \quad (6.3)$$

where, $\Delta t_a = t_{ao} - t_{ai}$ and $\Delta t_c = t_{ci} - t_{co}$

Heat capacity rate for air side

$$C_a = \rho_a * W_c * H_c * u * c_{pa} \quad (6.4)$$

Heat capacity rate for coolant side

$$C_c = \rho_c * V_c * c_{pc} \quad (6.5)$$

Cooling effectiveness

$$\varepsilon = \frac{Q_{avg}}{C_{min} (C_a, C_c) * (T_{ci} - T_{ai})} \quad (6.6)$$

6.4 Evaluation of engine performance

Mass of fuel consumption rate

$$m_f = V * \rho / t \quad (6.7)$$

Brake power of the engine

$$BP = \frac{W * N}{2200} * 0.746 \quad (6.8)$$

Brake Specific Fuel consumption

$$BSFC = \frac{m_f}{BP} \quad (6.9)$$

Indicated power of the engine

$$IP = FP + BP \quad (6.10)$$

Mechanical Efficiency of the engine

$$\eta_m = \frac{BP}{IP} \quad (6.11)$$

Brake thermal efficiency of the engine

$$\eta_{bth} = \frac{BP}{m_f * CV} * 100 \quad (6.12)$$

Indicated thermal efficiency of the engine

$$\eta_{ith} = \frac{IP}{m_f * CV} \quad (6.13)$$

6.5 Experimental Uncertainties

During experiments with radiators, the temperatures, flow rates, velocities and pressure loss were measured with appropriate instruments. During the measurement of parameters, the uncertainties occurred for the radiator are presented in Table 5.4 and the total uncertainties found in estimated results for radiator are given in Table 5.5 of Chapter 5. For the engine, the load, rpm and fuel consumption were measured with appropriate instruments and the uncertainties

values are within $\pm 0.25\%$. However, the total uncertainties value found for engine performance BP and IP are within the limit of 8 %. Repeatability test shows that the all sets of experiment data are within the uncertainty limits.

6.6 Results and Discussions

Based on the various load applied to the Kirloskar CI engine through hydraulic dynamometer, the fuel consumption rate and the brake specific fuel consumption in kg/hr has been calculated. Indicated power developed by the engine has been plotted as shown in Fig. 6.5, with the help of Willian's line. With the increase in engine load mass of fuel consumption increases and the total indicated power of the engine can be calculated by both friction power and engine brake power.

6.6.1 Performance evaluation with water, PG brine and EG brine coolants

Variations in effectiveness, heat transfer rate of radiator for water, PG brine and EG with engine performance are shown in Figs.6.6-6.7. Effectiveness of PG brine as radiator coolant decreases by 1% and increases by 5% with respect to water and 25% EG brine respectively, at engine full load condition. Coolant effectiveness increases with increase in engine load as higher temperature heated the walls of the cylinder and coolants in contact with them caused higher effectiveness in radiator through convective heat transfer medium.

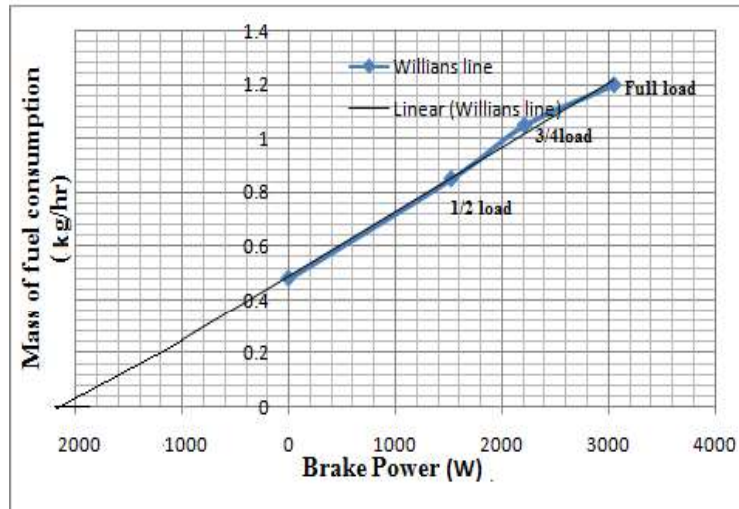


Figure 6.5: Indicated Power from Willian's line

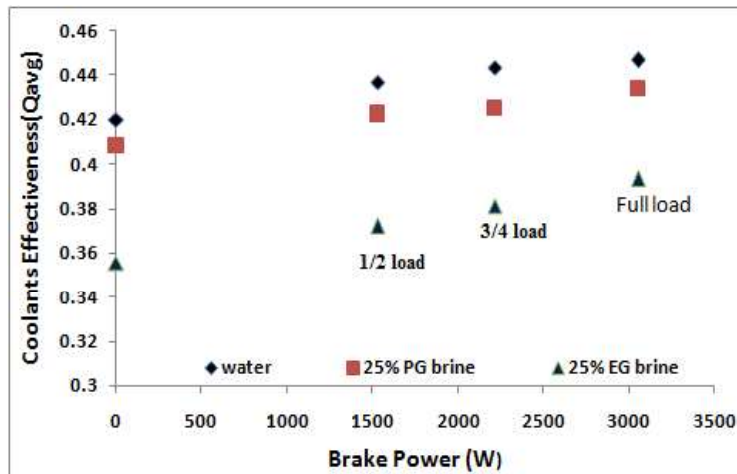


Figure 6.6: Engine brake power with coolants effectiveness

However, both 25% PG brine and water have nearly similar performance of effectiveness as compared to 25% EG brine as radiator coolants. Heat transfer rate in radiator for PG brine as radiator coolant decreases by 1.2% and increases by 12.1% with respect to water and 25% EG brine respectively, at engine full load condition and coolant flow rate of 6lpm through the radiator flat tube of hydraulic diameter of 0.002 m. Also heat transfer rate increases with increase in engine indicated power for a frontal air velocity of 4.5m/s. The combustion temperature

inside the engine increases due to higher load and coolants contact to cylinder wall may cause the higher heat transfer rate in radiator through convective heat transfer medium.

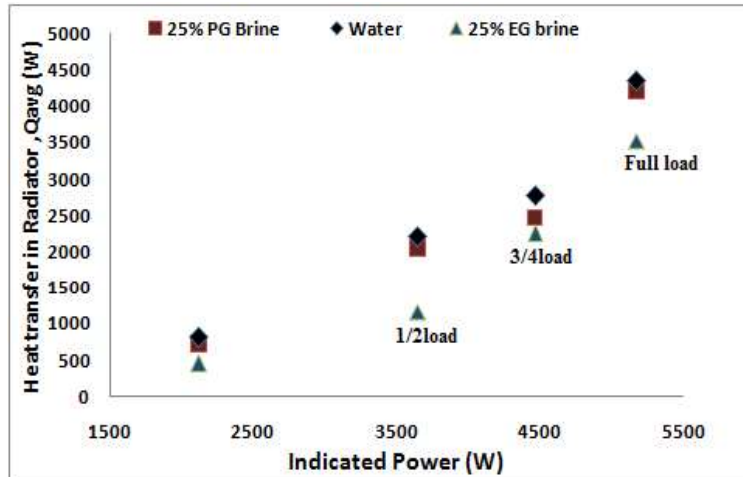


Figure 6.7: Engine indicated power with radiator heat transfer

Variation in coolant side heat transfer rate, coolant exit temperature and air side heat transfer rate are shown in Figs. 6.8-6.10. Coolant side heat transfer rate in radiator for PG brine decreases 5% and increases 13.2% with respect to water and 25% EG brine respectively, at engine full load condition. Due to higher heat transfer coefficient of PG brine coolants, it results in higher performance as compared to water and EG brine. Coolant exit temperature in radiator for PG brine increases by 1.6% and decreases by 8.6% with respect to water and 25% EG brine respectively, at engine full load condition. Increase in thermal efficiency tends to increase the combustion temperature inside the cylinder which results in increase of coolant temperature difference between the inlet and outlet zone. Also, due to higher heat transfer coefficient of PG brine coolants, it results in higher performance as compared to water and EG brine.

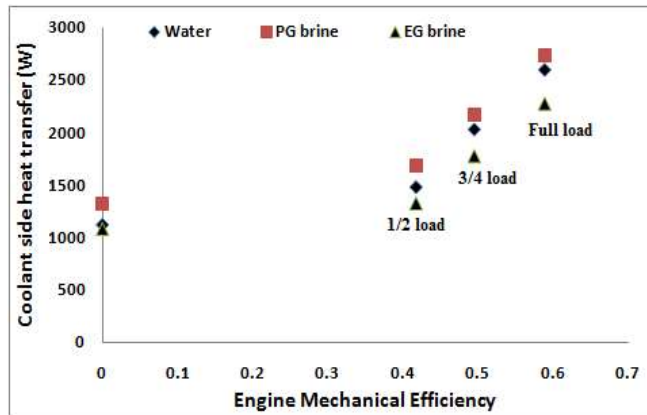


Figure 6.8: Coolant side heat transfer with η_m

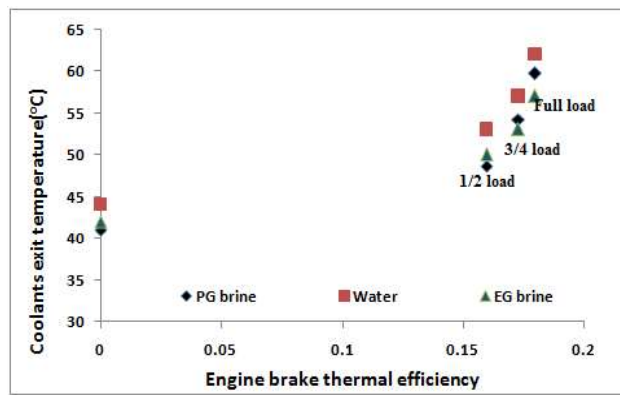


Figure 6.9: Coolant exit temperature with η_{bth}

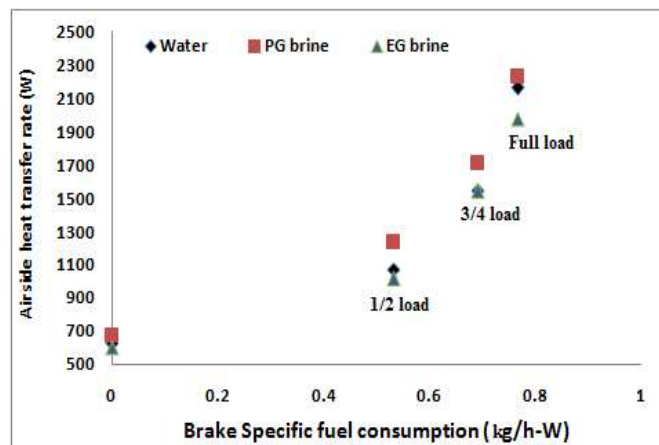


Figure 6.10: Air side heat transfer rate with BSFC

Air side heat transfer rate in radiator for PG brine increases by 4.48% and 11.78% with respect to water and 25% EG brine respectively, at engine full load

IIT (BHU), Varanasi Page 139

condition and air side heat transfer rate increases with increase in brake specific fuel consumption. Increase in brake specific fuel consumption tends to increase the combustion temperature inside the cylinder which results the increase in air side heat transfer rate.

6.6.2 Performance evaluation with PG and EG brine based nanofluid and hybrid nanofluids coolants.

Variations in effectiveness and heat transfer rate of radiator with Al_2O_3 +PG brine, EG brine based Al_2O_3 nanofluid and PG brine based ($0.5\%\text{Al}_2\text{O}_3+0.5\%\text{TiO}_2$) hybrid nanofluid are shown in Figs.6.11-6.12. Effectiveness of (PG brine+ Al_2O_3) nanofluid as radiator coolant is 1.2 % lower and 4.48% higher than that of PG brine based ($0.5\%\text{Al}_2\text{O}_3+0.5\%\text{TiO}_2$) hybrid nanofluid and (Al_2O_3 +EG brine) respectively, at engine full load condition. Also coolant effectiveness increases with increase in engine load due to the heated walls of the cylinder, which lead to heat the radiator coolants.

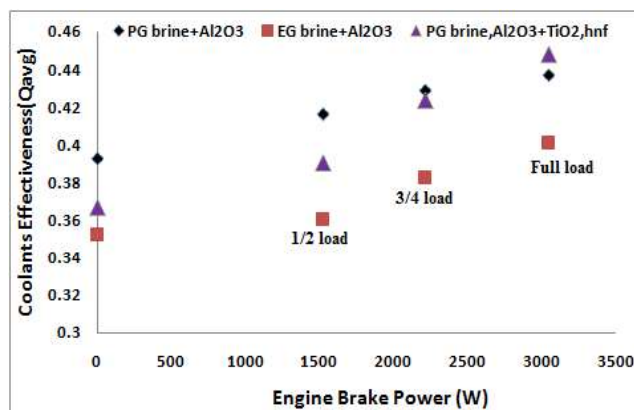


Figure 6.11: Coolants effectiveness with Engine brake power

Heat transfer rate in radiator for PG brine based Al_2O_3 nanofluid as radiator coolant decreases by 3.2% and increases by 7.4% with respect to PG brine based ($0.5\%\text{Al}_2\text{O}_3+0.5\%\text{TiO}_2$) hybrid nanofluid and (25% EG brine+ Al_2O_3) nanofluid respectively, at engine full load condition and coolant flow rate of

8l/min through the radiator flat tube of hydraulic diameter of 0.002m. As shown, heat transfer rate increases with increase in engine indicated power with a frontal air velocity of 4.5m/s. Combustion temperature inside the engine increases with higher load, which may leads to higher the heat transfer rate in radiator through the coolant contact surfaces.

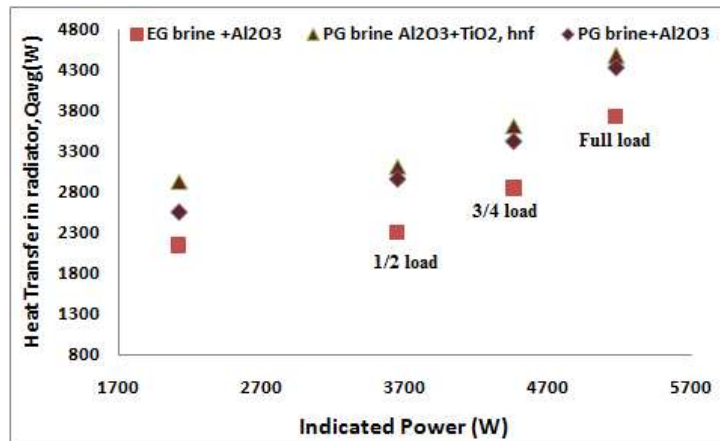


Figure 6.12: Engine indicated power with radiator heat transfer

Variations in coolant side heat transfer rate, coolant exit temperature and air side heat transfer rate are shown in (Fig.6.13-6.15). At engine full load condition, the coolant side heat transfer rate in radiator for PG brine based Al₂O₃ nanofluid decreases by 5% and increases by 8% for (0.5%Al₂O₃+0.5%TiO₂)/25% PG brine hybrid nanofluid and Al₂O₃/25%EG brine nanofluid, respectively. Coolant exit temperature in radiator for PG brine based Al₂O₃ nanofluid as radiator coolant decreases by 1.5% and increases by 5.8% with respect to PG brine based (0.5%Al₂O₃+0.5%TiO₂) hybrid nanofluid and (25% EG brine+ Al₂O₃) nanofluid respectively, at engine full load condition. Air side heat transfer rate in radiator for PG brine based Al₂O₃ nanofluid as radiator coolant decreases by 4.9% and increases by 15.3% with respect to PG brine based (0.5%Al₂O₃+0.5%TiO₂)

hybrid nanofluid and (25% EG brine+ Al₂O₃) nanofluid respectively, at engine full load condition.

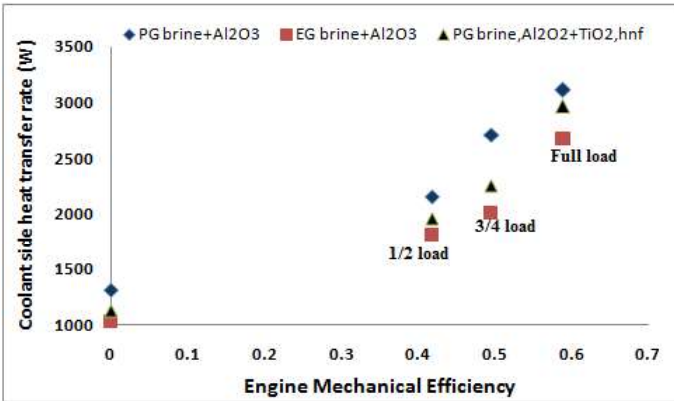


Figure 6.13: Coolant side heat transfer with η_m

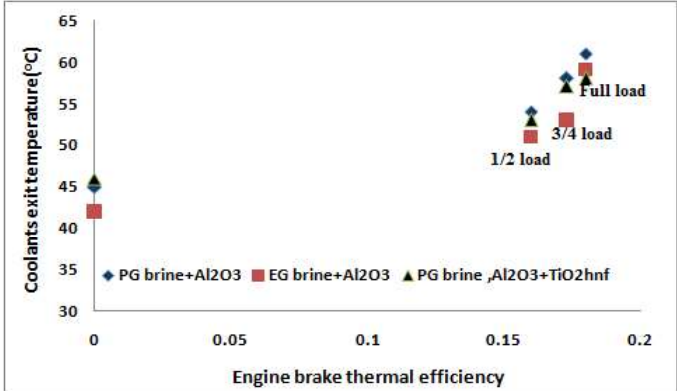


Figure 6.14: Coolant exit temperature with η_{bth}

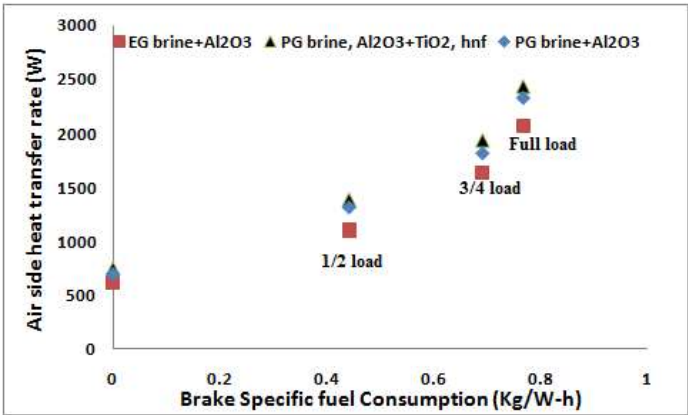


Figure 6.15 : Air side heat transfer with BSFC

Further air side heat transfer rate increases with increase in brake specific fuel consumption. Increase in brake specific fuel consumption tends to increase the combustion temperature inside the cylinder which results the increase in air side heat transfer rate.

6.7 Effect of cost, weight and space

By changing the different coolants in radiator, the radiator size is also affected with the engine load as shown in (Fig.6.16- 6.17). Experimental results show that by the application of full load to the engine and for the same heat transfer rate with compared to conventional coolant (25% EG brine) radiator core volume size decreases by 10%, 8% and 5% for PG brine based hybrid nanofluid, PG brine based nanofluid and 25%PG brine, respectively. Reduction in radiator size can reduce the material of tubes and fins, which will ultimately lead to the reduction in overall cost of the system. So a compact and lighter heat exchanger/radiator system can be designed with same heat transfer capacity.

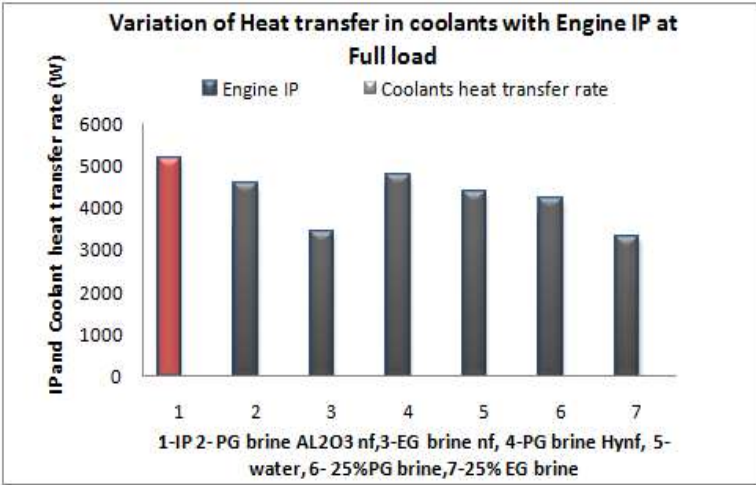


Figure 6.16: Comparison of coolant heat transfer rate with IP

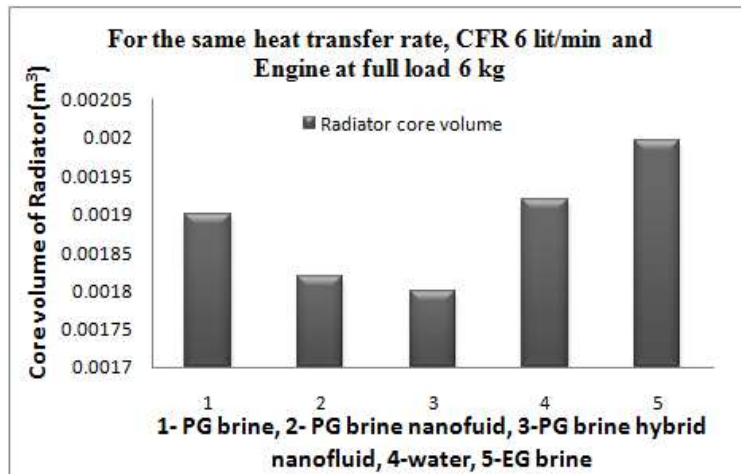


Figure 6.17: Radiator size variation for different coolants

6.8 Fuel energy distribution results

Experimental results of Fuel energy distributions with various coolants, at engine full load condition are shown in Figs.6.18-6.20. Results show that, from the supplied 100% of fuel energy, 29%, 31.4% and 33.2% have been losses for water, PG brine based nanofluid and PG brine based hybrid nanofluid respectively radiator coolant to cool the engine for smooth running.

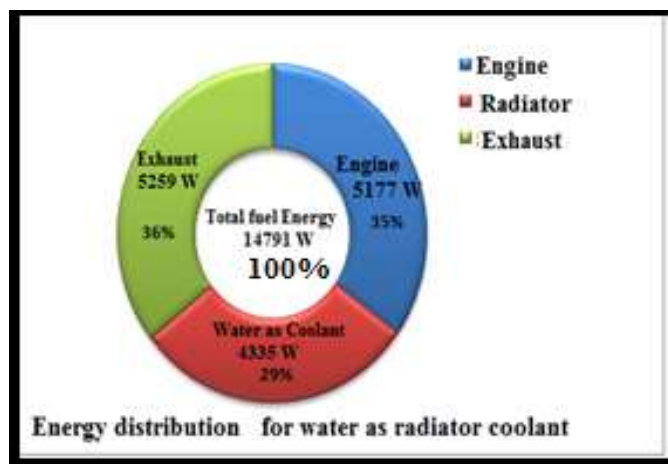


Figure 6.18: Fuel energy distribution water as coolant

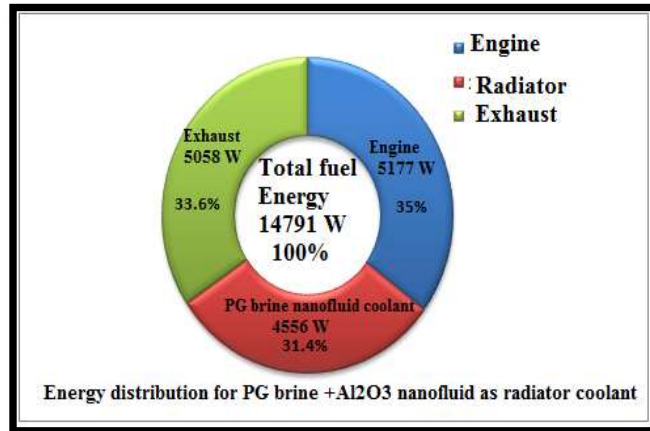


Figure 6.19 : Fuel energy distribution PG brine based nanofluid

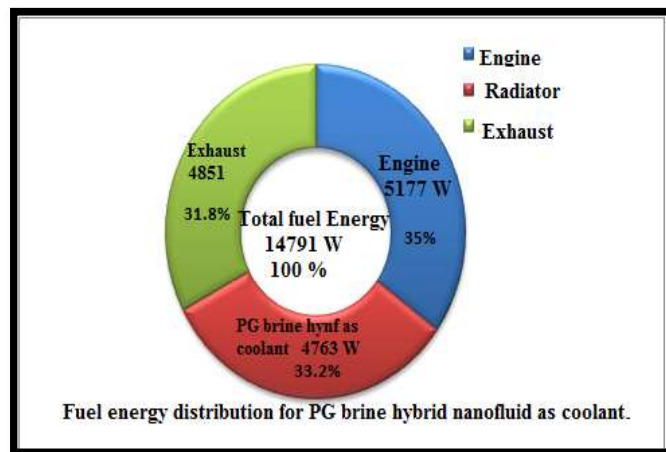


Figure 6.20 : Fuel energy distribution PG brine based hybrid

With constant engine power output, the increase in heat loss through various coolants result, decrease in the exhaust emission which is benefit for environment. Results show that PG brine based hybrid nanofluid has better coolant performance as compared to all above mentioned coolants as 33.2% heat loss carried through this coolant results in exhaust emission of 31.8% which is benefit to the environment.